Measurement of the inclusive branching fraction for $\psi(3686) \to K_S^0 + anything$

BESIII Collaboration [*]

M. Ablikim [a], M.N. Achasov [j,2], P. Adlarson [br], S. Ahmed [o], M. Albrecht [d], R. Aliberti [ae], A. Amoroso [bo,bq], Q. An [bl,ax], X.H. Bai [bf], Y. Bai [aw], O. Bakina [af], R. Baldini Ferroli [w], I. Balossino [z], Y. Ban [an,8], K. Begzsuren [ac], J.V. Bennett [e], N. Berger [ae], M. Bertani [w], D. Bettoni [z], F. Bianchi [bo,bq], J. Biernat [br], J. Bloms [bi], A. Bortone [bo,bq], I. Boyko [af], R.A. Briere [e], H. Cai [bs], X. Cai [a,ax], A. Calcaterra [w], G.F. Cao [a,bc], N. Cao [a,bc], S.A. Cetin [ba], J.F. Chang [a,ax], W.L. Chang [a,bc], G. Chelkov [af,1], D.Y. Chen [f], G. Chen [a], H.S. Chen [a,bc], M.L. Chen [a,ax], S.J. Chen [al], X.R. Chen [ab], Y.B. Chen [a,ax], Z.J. Chen [t,9], W.S. Cheng [bq], G. Cibinetto [z], F. Cossio [bq], X.F. Cui [am], H.L. Dai [a,ax], X.C. Dai [a,bc], A. Dbeyssi [o], R.E. de Boer [d], D. Dedovich [af], Z.Y. Deng [a], A. Denig [ae], I. Denysenko [af], M. Destefanis [bo,bq], F. De Mori [bo,bq], Y. Ding [aj], C. Dong [am], J. Dong [a,ax], L.Y. Dong [a,bc], M.Y. Dong [a,ax,bc], S.X. Du [bv], J. Fang [a,ax], S.S. Fang [a,bc], Y. Fang [a], R. Farinelli [z], L. Fava [bp,bq], F. Feldbauer [d], G. Felici [w], C.Q. Feng [bl,ax], M. Fritsch [d], C.D. Fu [a], Y. Fu [a], X.L. Gao [bl,ax], Y. Gao [bl,ax], Y. Gao [bm], Y. Gao [an,8], Y.G. Gao [f], I. Garzia [z,aa], E.M. Gersabeck [bg], A. Gilman [bh], K. Goetzen [k], L. Gong [aj], W.X. Gong [a,ax], W. Gradl [ae], M. Greco [bo,bq], L.M. Gu [al], M.H. Gu [a,ax], S. Gu [b], Y.T. Gu [m], C.Y. Guan [a,bc], A.Q. Guo [v], L.B. Guo [ak], R.P. Guo [ap], Y.P. Guo [i,6], A. Guskov [af,1], S. Han [bs], T.T. Han [aq], T.Z. Han [i,6], X.Q. Hao [p], F.A. Harris [be], K.L. He [a,bc], F.H. Heinsius [d], C.H. Heinz [ae], T. Held [d], Y.K. Heng [a,ax,bc], M. Himmelreich [k,4], T. Holtmann [d], Y.R. Hou [bc], Z.L. Hou [a], H.M. Hu [a,bc], J.F. Hu [ar,5], T. Hu [a,ax,bc], Y. Hu [a], G.S. Huang [bl,ax], L.Q. Huang [bm], X.T. Huang [aq], Y.P. Huang [a], Z. Huang [an,8], T. Hussain [bn], N. Hüsken [bi], W. Ikegami Andersson [br], W. Imoehl [v], M. Irshad [bl,ax], S. Jaeger [d], S. Janchiv [ac], Q. Ji [a], Q.P. Ji [p], X.B. Ji [a,bc], X.L. Ji [a,ax], H.B. Jiang [aq], X.S. Jiang [a,ax,bc], J.B. Jiao [aq], Z. Jiao [r], S. Jin [al], Y. Jin [bf], T. Johansson [br], N. Kalantar-Nayestanaki [bd], X.S. Kang [aj], R. Kappert [bd], M. Kavatsyuk [bd], B.C. Ke [as,a], I.K. Keshk [d], A. Khoukaz [bi], P. Kiese [ae], R. Kiuchi [a], R. Kliemt [k], L. Koch [ag], O.B. Kolcu [ba,12], B. Kopf [d], M. Kuemmel [d], M. Kuessner [d], A. Kupsc [br], M.G. Kurth [a,bc], W. Kühn [ag], J.J. Lane [bg], J.S. Lange [ag], P. Larin [o], A. Lavania [u], L. Lavezzi [bo,bq], H. Leithoff [ae], M. Lellmann [ae], T. Lenz [ae],

C. Li [ao], C.H. Li [ai], Cheng Li [bl,ax], D.M. Li [bv], F. Li [a,ax], G. Li [a], H. Li [as], H. Li [bl,ax], H.B. Li [a,bc], H.J. Li [i,6], J.L. Li [aq], J.Q. Li [d], Ke Li [a], L.K. Li [a], Lei Li [c], P.L. Li [bl,ax], P.R. Li [ah,10,11], S.Y. Li [az], W.D. Li [a,bc], W.G. Li [a], X.H. Li [bl,ax], X.L. Li [aq], Z.Y. Li [ay], H. Liang [a,bc], H. Liang [bl,ax], Y.F. Liang [au], Y.T. Liang [ab], G.R. Liao [l], L.Z. Liao [a,bc], J. Libby [u], C.X. Lin [ay], B. Liu [ar,5], B.J. Liu [a], C.X. Liu [a], D. Liu [bl,ax], D.Y. Liu [ar,5], F.H. Liu [at], Fang Liu [a], Feng Liu [f], H.B. Liu [m], H.M. Liu [a,bc], Huanhuan Liu [a], Huihui Liu [q], J.B. Liu [bl,ax], J.Y. Liu [a,bc], K. Liu [a], K.Y. Liu [aj], L. Liu [bl,ax], Q. Liu [bc], S.B. Liu [bl,ax], Shuai Liu [av], T. Liu [a,bc], W.M. Liu [bl,ax], X. Liu [ah,10,11], Y.B. Liu [am], Z.A. Liu [a,ax,bc], Z.Q. Liu [aq], X.C. Lou [a,ax,bc], F.X. Lu [p], H.J. Lu [r], J.D. Lu [a,bc], J.G. Lu [a,ax], X.L. Lu [a], Y. Lu [a], Y.P. Lu [a,ax], C.L. Luo [ak], M.X. Luo [bu], P.W. Luo [ay], T. Luo [i,6], X.L. Luo [a,ax], S. Lusso [bq], X.R. Lyu [bc], F.C. Ma [aj], H.L. Ma [a], L.L. Ma [aq], M.M. Ma [a,bc], Q.M. Ma [a], R.Q. Ma [a,bc], R.T. Ma [bc], X.N. Ma [am], X.X. Ma [a,bc], X.Y. Ma [a,ax], Y.M. Ma [aq], F.E. Maas [o], M. Maggiora [bo,bq], S. Maldaner [d], S. Malde [bj], Q.A. Malik [bn], A. Mangoni [x], Y.J. Mao [an,8], Z.P. Mao [a], S. Marcello [bo,bq], Z.X. Meng [bf], J.G. Messchendorp [bd], G. Mezzadri [z], T.J. Min [al], R.E. Mitchell [v], X.H. Mo [a,ax,bc], N.Yu. Muchnoi [j,2], H. Muramatsu [bh], S. Nakhoul [k,4], Y. Nefedov [af], F. Nerling [k,4], I.B. Nikolaev [j,2], Z. Ning [a,ax], S. Nisar [h,7], S.L. Olsen [bc], Q. Ouyang [a,ax,bc], S. Pacetti [x,y], X. Pan [i,6], Y. Pan [bg], A. Pathak [a], P. Patteri [w], M. Pelizaeus [d], H.P. Peng [bl,ax], K. Peters [k,4], J. Pettersson [br], J.L. Ping [ak], R.G. Ping [a,bc], A. Pitka [d], R. Poling [bh], V. Prasad [bl,ax], H. Qi [bl,ax], H.R. Qi [az], M. Qi [al], T.Y. Qi [b], T.Y. Qi [i], S. Qian [a,ax], W.B. Qian [bc], Z. Qian [ay], C.F. Qiao [bc], L.Q. Qin [l], X.S. Qin [d], Z.H. Qin [a,ax], J.F. Qiu [a], S.Q. Qu [am], K.H. Rashid [bn], K. Ravindran [u], C.F. Redmer [ae], A. Rivetti [bq], V. Rodin [bd], M. Rolo [bq], G. Rong [a,bc], Ch. Rosner [o], M. Rump [bi], A. Sarantsev [af,3], Y. Schelhaas [ae], C. Schnier [d], K. Schoenning [br], M. Scodeggio [z,aa], D.C. Shan [av], W. Shan [s], X.Y. Shan [bl,ax], M. Shao [bl,ax], C.P. Shen [i], P.X. Shen [am], X.Y. Shen [a,bc], H.C. Shi [bl,ax], R.S. Shi [a,bc], X. Shi [a,ax], X.D. Shi [bl,ax], J.J. Song [aq], Q.Q. Song [bl,ax], W.M. Song [ad,a], Y.X. Song [an,8], S. Sosio [bo,bq], S. Spataro [bo,bq], F.F. Sui [aq], G.X. Sun [a], J.F. Sun [p], L. Sun [bs], S.S. Sun [a,bc], T. Sun [a,bc], W.Y. Sun [ak], X. Sun [t,9], Y.J. Sun [bl,ax], Y.K. Sun [bl,ax], Y.Z. Sun [a], Z.T. Sun [a], Y.H. Tan [bs], Y.X. Tan [bl,ax], C.J. Tang [au], G.Y. Tang [a], J. Tang [ay], J.X. Teng [bl,ax], V. Thoren [br], I. Uman [bb], B. Wang [a], B.L. Wang [bc], C.W. Wang [al], D.Y. Wang [an,8], H.P. Wang [a,bc], K. Wang [a,ax], L.L. Wang [a], M. Wang [aq], M.Z. Wang [an,8], Meng Wang [a,bc], W.H. Wang [bs], W.P. Wang [bl,ax], X. Wang [an,8], X.F. Wang [ah,10,11], X.L. Wang [i,6], Y. Wang [ay], Y. Wang [bl,ax], Y.D. Wang [o], Y.F. Wang [a,ax,bc], Y.Q. Wang [a], Z. Wang [a,ax], Z.Y. Wang [a], Ziyi Wang [bc], Zongyuan Wang [a,bc], D.H. Wei [l], P. Weidenkaff [ae], F. Weidner [bi], S.P. Wen [a], D.J. White [bg], U. Wiedner [d], G. Wilkinson [bj], M. Wolke [br], L. Wollenberg [d], J.F. Wu [a,bc], L.H. Wu [a], L.J. Wu [a,bc], X. Wu [i,6], Z. Wu [a,ax], L. Xia [bl,ax], H. Xiao [i,6], S.Y. Xiao [a], Y.J. Xiao [a,bc], Z.J. Xiao [ak], X.H. Xie [an,8], Y.G. Xie [a,ax], Y.H. Xie [f], T.Y. Xing [a,bc], X.A. Xiong [a,bc], G.F. Xu [a], J.J. Xu [al], Q.J. Xu [n], W. Xu [a,bc], X.P. Xu [av], Y.C. Xu [bc], F. Yan [i,6], L. Yan [bo,bq], L. Yan [i,6], W.B. Yan [bl,ax], W.C. Yan [bv], Xu Yan [av], H.J. Yang [ar,5], H.X. Yang [a], L. Yang [bs], R.X. Yang [bl,ax], S.L. Yang [a,bc], Y.H. Yang [al], Y.X. Yang [l], Yifan Yang [a,bc], Zhi Yang [ab], M. Ye [a,ax], M.H. Ye [g], J.H. Yin [a], Z.Y. You [ay], B.X. Yu [a,ax,bc], C.X. Yu [am], G. Yu [a,bc], J.S. Yu [t,9], T. Yu [bm], C.Z. Yuan [a,bc], W. Yuan [bo,bq], X.Q. Yuan [an,8], Y. Yuan [a], Z.Y. Yuan [ay], C.X. Yue [ai], A.A. Zafar [bn], Y. Zeng [t,9], B.X. Zhang [a], Guangyi Zhang [p], H. Zhang [bl], H.H. Zhang [ay], H.Y. Zhang [a,ax], J.L. Zhang [bt], J.Q. Zhang [ak], J.Q. Zhang [d], J.W. Zhang [a,ax,bc], J.Y. Zhang [a], J.Z. Zhang [a,bc], Jianyu Zhang [a,bc], Jiawei Zhang [a,bc], Lei Zhang [al], S. Zhang [ay], S.F. Zhang [al], T.J. Zhang [ar,5], X.Y. Zhang [aq], Y. Zhang [bj], Y.H. Zhang [a,ax], Y.T. Zhang [bl,ax], Yan Zhang [bl,ax], Yao Zhang [a], Yi Zhang [i,6], Z.Y. Zhang [bs], G. Zhao [a], J. Zhao [ai], J.Y. Zhao [a,bc], J.Z. Zhao [a,ax], Lei Zhao [bl,ax], Ling Zhao [a], M.G. Zhao [am], Q. Zhao [a], S.J. Zhao [bv], Y.B. Zhao [a,ax], Y.X. Zhao [ab], Z.G. Zhao [bl,ax], A. Zhemchugov [af,1], B. Zheng [bm], J.P. Zheng [a,ax], Y.H. Zheng [bc], B. Zhong [ak], C. Zhong [bm], L.P. Zhou [a,bc], Q. Zhou [a,bc], X. Zhou [bs], X.K. Zhou [bc], X.R. Zhou [bl,ax], A.N. Zhu [a,bc], J. Zhu [am], K. Zhu [a], K.J. Zhu [a,ax,bc], S.H. Zhu [bk], W.J. Zhu [am], Y.C. Zhu [bl,ax], Z.A. Zhu [a,bc], B.S. Zou [a], J.H. Zou [a]

[a] Institute of High Energy Physics, Beijing 100049, People's Republic of China
[b] Beihang University, Beijing 100191, People's Republic of China
[c] Beijing Institute of Petrochemical Technology, Beijing 102617, People's Republic of China
[d] Bochum Ruhr-University, D-44780 Bochum, Germany
[e] Carnegie Mellon University, Pittsburgh, PA 15213, USA

[f] *Central China Normal University, Wuhan 430079, People's Republic of China*
[g] *China Center of Advanced Science and Technology, Beijing 100190, People's Republic of China*
[h] *COMSATS University Islamabad, Lahore Campus, Defence Road, Off Raiwind Road, 54000 Lahore, Pakistan*
[i] *Fudan University, Shanghai 200443, People's Republic of China*
[j] *G.I. Budker Institute of Nuclear Physics SB RAS (BINP), Novosibirsk 630090, Russia*
[k] *GSI Helmholtzcentre for Heavy Ion Research GmbH, D-64291 Darmstadt, Germany*
[l] *Guangxi Normal University, Guilin 541004, People's Republic of China*
[m] *Guangxi University, Nanning 530004, People's Republic of China*
[n] *Hangzhou Normal University, Hangzhou 310036, People's Republic of China*
[o] *Helmholtz Institute Mainz, Staudinger Weg 18, D-55099 Mainz, Germany*
[p] *Henan Normal University, Xinxiang 453007, People's Republic of China*
[q] *Henan University of Science and Technology, Luoyang 471003, People's Republic of China*
[r] *Huangshan College, Huangshan 245000, People's Republic of China*
[s] *Hunan Normal University, Changsha 410081, People's Republic of China*
[t] *Hunan University, Changsha 410082, People's Republic of China*
[u] *Indian Institute of Technology Madras, Chennai 600036, India*
[v] *Indiana University, Bloomington, IN 47405, USA*
[w] *INFN Laboratori Nazionali di Frascati, I-00044, Frascati, Italy*
[x] *INFN Sezione di Perugia, I-06100, Perugia, Italy*
[y] *University of Perugia, I-06100, Perugia, Italy*
[z] *INFN Sezione di Ferrara, I-44122, Ferrara, Italy*
[aa] *University of Ferrara, I-44122, Ferrara, Italy*
[ab] *Institute of Modern Physics, Lanzhou 730000, People's Republic of China*
[ac] *Institute of Physics and Technology, Peace Ave. 54B, Ulaanbaatar 13330, Mongolia*
[ad] *Jilin University, Changchun 130012, People's Republic of China*
[ae] *Johannes Gutenberg University of Mainz, Johann-Joachim-Becher-Weg 45, D-55099 Mainz, Germany*
[af] *Joint Institute for Nuclear Research, 141980 Dubna, Moscow region, Russia*
[ag] *Justus-Liebig-Universitaet Giessen, II. Physikalisches Institut, Heinrich-Buff-Ring 16, D-35392 Giessen, Germany*
[ah] *Lanzhou University, Lanzhou 730000, People's Republic of China*
[ai] *Liaoning Normal University, Dalian 116029, People's Republic of China*
[aj] *Liaoning University, Shenyang 110036, People's Republic of China*
[ak] *Nanjing Normal University, Nanjing 210023, People's Republic of China*
[al] *Nanjing University, Nanjing 210093, People's Republic of China*
[am] *Nankai University, Tianjin 300071, People's Republic of China*
[an] *Peking University, Beijing 100871, People's Republic of China*
[ao] *Qufu Normal University, Qufu 273165, People's Republic of China*
[ap] *Shandong Normal University, Jinan 250014, People's Republic of China*
[aq] *Shandong University, Jinan 250100, People's Republic of China*
[ar] *Shanghai Jiao Tong University, Shanghai 200240, People's Republic of China*
[as] *Shanxi Normal University, Linfen 041004, People's Republic of China*
[at] *Shanxi University, Taiyuan 030006, People's Republic of China*
[au] *Sichuan University, Chengdu 610064, People's Republic of China*
[av] *Soochow University, Suzhou 215006, People's Republic of China*
[aw] *Southeast University, Nanjing 211100, People's Republic of China*
[ax] *State Key Laboratory of Particle Detection and Electronics, Beijing 100049, Hefei 230026, People's Republic of China*
[ay] *Sun Yat-Sen University, Guangzhou 510275, People's Republic of China*
[az] *Tsinghua University, Beijing 100084, People's Republic of China*
[ba] *Istanbul Bilgi University, HEP Res. Cent., 34060 Eyup, Istanbul, Turkey*
[bb] *Near East University, Nicosia, North Cyprus, Mersin 10, Turkey*
[bc] *University of Chinese Academy of Sciences, Beijing 100049, People's Republic of China*
[bd] *University of Groningen, NL-9747 AA Groningen, The Netherlands*
[be] *University of Hawaii, Honolulu, HI 96822, USA*
[bf] *University of Jinan, Jinan 250022, People's Republic of China*
[bg] *University of Manchester, Oxford Road, Manchester, M13 9PL, United Kingdom*
[bh] *University of Minnesota, Minneapolis, MN 55455, USA*
[bi] *University of Muenster, Wilhelm-Klemm-Str. 9, 48149 Muenster, Germany*
[bj] *University of Oxford, Keble Rd, Oxford, OX13RH, United Kingdom*
[bk] *University of Science and Technology Liaoning, Anshan 114051, People's Republic of China*
[bl] *University of Science and Technology of China, Hefei 230026, People's Republic of China*
[bm] *University of South China, Hengyang 421001, People's Republic of China*
[bn] *University of the Punjab, Lahore-54590, Pakistan*
[bo] *University of Turin, I-10125, Turin, Italy*
[bp] *University of Eastern Piedmont, I-15121, Alessandria, Italy*
[bq] *INFN, I-10125, Turin, Italy*
[br] *Uppsala University, Box 516, SE-75120 Uppsala, Sweden*
[bs] *Wuhan University, Wuhan 430072, People's Republic of China*
[bt] *Xinyang Normal University, Xinyang 464000, People's Republic of China*
[bu] *Zhejiang University, Hangzhou 310027, People's Republic of China*
[bv] *Zhengzhou University, Zhengzhou 450001, People's Republic of China*

ARTICLE INFO

ABSTRACT

Using 5.9 pb^{-1} of e^+e^- annihilation data collected at center-of-mass energies from 3.640 to 3.701 GeV with the BESIII detector at the BEPCII Collider, we measure the observed cross sections of $e^+e^- \to K_S^0 X$ (where $X =$ anything). From a fit to these observed cross sections with the sum of continuum and $\psi(3686)$ and J/ψ Breit-Wigner functions and considering initial state radiation and the BEPCII beam energy spread, we obtain for the first time the product of $\psi(3686)$ leptonic width and inclusive decay

branching fraction $\Gamma_{\psi(3686)}^{ee}\mathcal{B}(\psi(3686) \to K_S^0 X) = (373.8 \pm 6.7 \pm 20.0)$ eV, and assuming $\Gamma_{\psi(3686)}^{ee}$ is (2.33 ± 0.04) keV from PDG value, we measure $\mathcal{B}(\psi(3686) \to K_S^0 X) = (16.04 \pm 0.29 \pm 0.90)\%$, where the first uncertainty is statistical and the second is systematic.

1. Introduction

The decays of $\psi(3686)$ provide an ideal laboratory to study the strong interaction between the charm quark and antiquark in the low energy region. The decay rates of $\psi(3686)$ to some exclusive final states can be predicted [1] by effective theories based on Quantum Chromodynamics (QCD). Although the $\psi(3686)$ decays have been studied for more than 40 years since its discovery in 1974 [2], the sum of the branching fractions (BFs) for all the decay channels in the PDG [3] is only approximately 90%, indicating that there are still many decay modes missing. Searching for new exclusive decay channels and measuring their BFs is important to test the QCD calculations of $\psi(3686)$ decays, which can lead to better understanding of the strong interaction in the low energy region.

Measurements of the BFs of inclusive $\psi(3686)$ decays, which include transitions, radiative decays, and hadronic decays, can guide the search for new exclusive decay modes, which could supply missing BFs for $\psi(3686)$ and other states, such as J/ψ and χ_{cJ} $(J = 0, 1, 2)$ produced in the $\psi(3686)$ transitions [4,5].

The K_S^0 is a long-lived particle, which is easily reconstructed in the detector, and it can be used as a probe to study the inclusive decays of $\psi(3686)$. In this paper, the BF of $\psi(3686) \to K_S^0 X$ ($X =$ anything) is measured for the first time by fitting the observed inclusive K_S^0 cross sections in e^+e^- annihilation in the $\psi(3686)$ energy region. The line-shape of the $\psi(3686)$ cross section is described by a Breit-Wigner function, in which the BF is a parameter [6].

2. Expected observed cross section

For $e^+e^- \to f$, where f are hadronic final states, the expected observed cross section, taking into consideration the initial state radiation (ISR) and the beam energy spread to describe the beam energy resolution, at a center-of-mass (c.m.) energy $\sqrt{s}$ is

$$\sigma^{\exp}(s) = \int_0^\infty ds' G(s, s') \int_0^1 dx \cdot \sigma^{\mathrm{Dress}}(s(1-x)) F(x, s), \qquad (1)$$

where x is the ratio of the total energy of the emitted photons to the beam energy [7] and $\sigma^{\mathrm{Dress}}(s)$ is the total dressed cross section for $e^+e^- \to f$, which includes the effects of vacuum polarization. For the resonances, such as J/ψ and $\psi(3686)$, the dressed cross section of $J/\psi \to f$ and $\psi(3686) \to f$ can be described by the Breit-Wigner formula; here, exactly the same parameterization as given in Ref. [6] is used:

$$\sigma^{\mathrm{Dress}}(s) = \frac{12\pi \Gamma^{ee} \Gamma^{\mathrm{tot}} \mathcal{B}(R \to f)}{(s - M^2)^2 + (\Gamma^{\mathrm{tot}} M)^2}, \qquad (2)$$

where M and Γ^{tot} are the mass and the total width of the resonance, Γ^{ee} is the partial width to the e^+e^- channel, and $\mathcal{B}(R \to f)$ is the BF for the resonance decay to the final state f. For the continuum, we assume that the dressed cross section has the energy dependence defined as

$$\sigma^{\mathrm{Dress}}(s) = \frac{f_{\mathrm{con}}}{s}, \qquad (3)$$

where f_{con} can be determined experimentally.

$F(x, s)$ is a sampling function based on the structure function approach by Kuraev and Fadin [7], given by

$$F(x, s) = \beta x^{\beta-1} \delta^{V+S} + \delta^H, \qquad (4)$$

where β is the electron equivalent radiator thickness,

$$\beta = \frac{2\alpha}{\pi}(L - 1), \qquad (5)$$

and

$$L = \ln \frac{s}{m_e^2}. \qquad (6)$$

Here, m_e is the mass of the electron and α is the fine structure constant. The correction term for the virtual process and a soft photon is

$$\delta^{V+S} = 1 + \frac{3}{4}\beta + \frac{\alpha}{\pi}(\frac{\pi^2}{3} - \frac{1}{2}) + \frac{\beta^2}{24}(\frac{37}{4} - \frac{L}{3} - 2\pi^2), \qquad (7)$$

and the correction term for the hard photon is

$$\delta^H = -\beta(1 - \frac{x}{2}) + \frac{1}{8}\beta^2[4(2 - x)\ln\frac{1}{x} - \frac{1 + 3(1-x)^2}{x}\ln(1-x) - 6 + x]. \qquad (8)$$

$G(s, s')$ is a Gaussian function to describe the beam energy spread. It is defined as

$$G(s, s') = \frac{1}{\sqrt{2\pi}\Delta}e^{-(\sqrt{s}-\sqrt{s'})^2/(2\Delta^2)}, \qquad (9)$$

where Δ is the standard deviation of the c.m. energy distribution, $\sqrt{s}$ and $\sqrt{s'}$ are the nominal and actual c.m. energies, respectively.

By fitting the observed cross section of $e^+e^- \to K_S^0 X$ as a function of c.m. energy with the sum of the expected continuum function and J/ψ and $\psi(3686)$ Breit-Wigner functions, the product of $\Gamma_{\psi(3686)}^{ee}$ and BF of $\psi(3686) \to K_S^0 X$ can be measured and taking PDG [3] value for $\Gamma_{\psi(3686)}^{ee}$, the BF of $\psi(3686) \to K_S^0 X$ is obtained. This approach has the advantage compared to directly measuring the BF at the $\psi(3686)$ resonance, where BESIII has a large data sample, of unfolding the continuum contribution from the resonance contribution and allowing the BF and cross section of $e^+e^- \to K_S^0 X$ to be determined at the same time.

3. Detector and Monte Carlo simulation

The BESIII detector is a magnetic spectrometer [8] located at the Beijing Electron Positron Collider (BEPCII) [9]. The cylindrical core of the BESIII detector consists of a helium-based multilayer drift chamber (MDC), a plastic scintillator time-of-flight system (TOF), and a CsI(Tl) electromagnetic calorimeter (EMC), which are all enclosed in a superconducting solenoidal magnet providing a 1.0 T magnetic field. The solenoid is supported by an octagonal flux-return yoke with resistive plate chamber muon identifier modules

Table 1
Numbers of signal MC events.

	$\sqrt{s}$ (GeV)	3.6451	3.6534	3.6789	3.6840	3.6860	3.6964
Signal	$\psi(3686) \to K_S^0 X$	111693	111337	111385	111441	111326	111224
MC	$J/\psi \to K_S^0 X$	101611	102237	101869	101489	101992	101988
samples	$e^+e^- \to K_S^0 X$	104595	105020	105097	104830	104778	105192

interleaved with steel. The acceptance of charged particles and photons is 93% over the 4π solid angle. The charged particle momentum resolution at 1 GeV/c is 0.5%, and the specific energy loss (dE/dx) resolution is 6% for the electrons from Bhabha scattering. The EMC measures photon energies with a resolution of 2.5% (5%) at 1 GeV in the barrel (end cap) region. The time resolution of the TOF barrel part is 68 ps, while that of the end cap part is 110 ps.

Three Monte Carlo (MC) simulated data samples ('inclusive MC') of $\psi(3686) \to$ anything, $J/\psi \to$ anything and $e^+e^- \to q\bar{q}$ ($q = u, d, s$) have been generated with KKMC [10] which simulates $\psi(3686)$, J/ψ and $q\bar{q}$ production in e^+e^- annihilation, while the subsequent decays of $\psi(3686)$ and J/ψ are handled by EVT-GEN [11]. For the known decay modes, the BFs are set to the world average values [3], while the remaining unknown decay modes are modeled by LUNDCHARM [12] in the EVTGEN generator. The simulated samples are produced with a GEANT4-based [13] MC software that includes the geometric description [14,15] of the BESIII detector and the detector response, and they are reconstructed to determine the detection efficiency and estimate the backgrounds. Each sample is generated with 600000 events for six energy points in the range from 3.645 GeV to 3.697 GeV to determine the efficiency dependence on the c.m. energy. The signal MC samples for $\psi(3686) \to K_S^0 X$, $J/\psi \to K_S^0 X$ and $e^+e^- \to K_S^0 X$ are selected with generator information from the inclusive MC samples of $\psi(3686)$, J/ψ and $e^+e^- \to q\bar{q}$, respectively. The numbers of events generated for each signal MC sample are summarized in Table 1 for the six energy points. To study the backgrounds, an inclusive MC sample of 1.06×10^8 $\psi(3686)$ events is used, referred to as "the standard $\psi(3686)$ inclusive MC sample" in the following. We also use samples of three QED processes, with $e^+e^- \to e^+e^-$ and $e^+e^- \to \mu^+\mu^-$ both generated by BABAYAGA [16], and $e^+e^- \to \tau^+\tau^-$ generated by KKMC [10].

In this analysis we use the $\psi(3686)$ cross-section scan data collected by BESIII in June 2010 at 22 energy points between 3.640 and 3.701 GeV with a total integrated luminosity of about 5.9 pb^{-1}. The c.m. energies and the corresponding integrated luminosities are listed in Table 2. In addition, the data sample of $(106.41 \pm 0.86) \times 10^6$ events [17] collected in 2009 at $\sqrt{s} = 3.686$ GeV is also used for a number of studies and is referred to as "the standard $\psi(3686)$ data" in the following.

4. Data analysis

4.1. Measurement of $\sigma^{\rm obs}(e^+e^- \to K_S^0 X)$

The $e^+e^- \to K_S^0 X$ candidate events, called inclusive K_S^0 events, are reconstructed using the most abundant K_S^0 decay to $\pi^+\pi^-$. More than two good charged tracks are required with $|\cos\theta| < 0.93$, $R_{xy} < 10$ cm, and $R_z < 20$ cm, where θ is the polar angle with respect to the z axis, while R_{xy} and R_z are the distances of the closest approach to the interaction point in the plane perpendicular to and along z, respectively. To select the K_S^0 daughter candidates, good charged tracks are assumed to be pions, and particle identification is not used. The candidates must satisfy the following selection criteria: (1) the total charge of the two tracks is zero; (2) the ratio E/p of each pion candidate is be less than 0.9 to reject electrons, where E is the energy deposited in the EMC and p is the momentum reconstructed in the MDC; (3) for each candidate pair, a secondary vertex fit [18] is performed; the decay length $L_{\rm decay}$
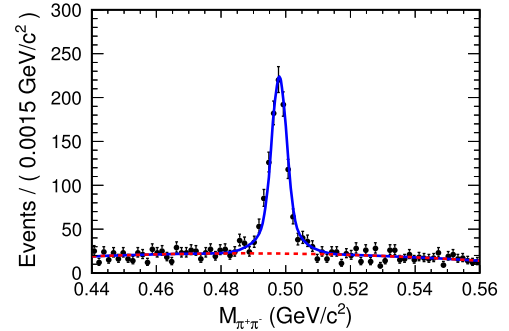

Fig. 1. The $\pi^+\pi^-$ invariant mass spectrum. Points with errors are scan sample data collected at $\sqrt{s}$ = 3.686 GeV. The blue solid line is the fit result, and the red dashed line represents the background contribution.

between the nominal interaction point and the secondary vertex is required to be larger than zero, and the combination with longest decay length ($L_{\rm max}$) is retained for further analysis. A further requirement, chosen by optimizing the ratio $S/\sqrt{S+B}$, where S and B are the numbers of signal and background events estimated from the standard $\psi(3686)$ inclusive MC sample, $L_{\rm max} > 0.4$ cm is applied. After the selection of the K_S^0 daughter candidates, at least one of the remaining good charged tracks is required to satisfy $R_{xy} < 1$ cm and $R_z < 10$ cm.

To obtain the signal yield at each energy point, we perform a maximum likelihood fit to the invariant mass spectrum of $\pi^+\pi^-$ with a Double-Gaussian function and a second-order Chebychev polynomial function, which are used to describe the signal and background, respectively. In the fit, the two Gaussian functions have a common mean value, and their parameters are fixed to the ones obtained by a fit to the $M_{\pi^+\pi^-}$ distribution from all data samples combined. As an example, Fig. 1 shows the fit result for the data set collected at $\sqrt{s} = 3.686$ GeV, where the K_S^0 signal is clearly seen. The yields of inclusive K_S^0 events, $N^{\rm obs}$, are obtained for each energy point and listed in Table 2.

The possible sources of background are $e^+e^- \to (\gamma)e^+e^-$, $e^+e^- \to (\gamma)\mu^+\mu^-$, $e^+e^- \to \tau^+\tau^-$ and non-K_S^0 events from $\psi(3686)$ decays. Among them, the only peaking background is $\psi(3686) \to K_L^0 + Y$, where Y can be anything except K_S^0. The number of these events ($N^{\rm bkg}$) is estimated by

$$N^{\rm bkg} = \mathcal{L} \times \eta^{\psi(3686) \to K_L^0 + Y} \times \sigma^{\psi(3686) \to K_L^0 + Y}, \qquad (10)$$

where $\mathcal{L}$ is the integrated luminosity of the data set and $\eta^{\psi(3686) \to K_L^0 + Y}$ is the probability to misidentify the $\psi(3686) \to K_L^0 + Y$ event as an inclusive K_S^0 event. The value $\eta^{\psi(3686) \to K_L^0 + Y} = (6.3 \pm 0.2) \times 10^{-4}$ is estimated from the inclusive MC samples. The observed cross section $\sigma^{\psi(3686) \to K_L^0 + Y}$ is calculated from Eq. (1)-(9), with the BF for $\psi(3686) \to K_L^0 + Y$ estimated using the standard $\psi(3686)$ inclusive MC sample, where known decays with K_L^0 are combined with those generated by LUNDCHARM [12]. At all energy points the estimated cross section $\sigma^{\psi(3686) \to K_L^0 + Y}$ is similar to the measured $\sigma^{\psi(3686) \to K_S^0 + X}$. The estimated number of peaking background events for each energy is reported in the fourth column of Table 2.

The detection efficiencies for the three signal processes are the ratios of the reconstructed events and the total number of events

Table 2
The values of the integrated luminosity, $\mathcal{L}$, the number of observed inclusive K_S^0 events, N^{obs}, the number of background events, N^{bkg}, the detection efficiency, $\epsilon^{e^+e^- \to K_S^0 X}$, the observed cross section, σ^{obs}, and the corresponding dress cross section, σ^{dress}, obtained at each c.m. energy point, $\sqrt{s}$.

| $\sqrt{s}$ (GeV)	$\mathcal{L}$ (nb^{-1})	N^{obs}	N^{bkg}	$\epsilon^{e^+e^- \to K_S^0 X}$ (%)	σ^{obs} (nb)	σ^{dress} (nb)
3.6451	568.7 ± 2.4	345.8 ± 27.1	0.0 ± 0.0	23.47 ± 0.05	2.59 ± 0.20	2.02 ± 0.16
3.6474	2260.9 ± 4.8	1465.3 ± 56.9	0.0 ± 0.0	23.47 ± 0.05	2.76 ± 0.11	2.15 ± 0.09
3.6534	2217.7 ± 4.8	1475.9 ± 55.7	0.0 ± 0.0	23.47 ± 0.05	2.84 ± 0.11	2.22 ± 0.09
3.6789	49.1 ± 0.7	34.6 ± 10.7	0.0 ± 0.0	23.31 ± 0.04	3.02 ± 0.93	2.60 ± 0.80
3.6799	46.5 ± 0.7	13.4 ± 9.6	0.0 ± 0.0	23.25 ± 0.04	1.24 ± 0.89	1.09 ± 0.78
3.6809	49.6 ± 0.7	58.9 ± 10.2	0.0 ± 0.0	23.12 ± 0.04	5.14 ± 0.89	4.53 ± 0.79
3.6818	52.2 ± 0.7	47.0 ± 9.5	0.0 ± 0.0	22.87 ± 0.03	3.94 ± 0.80	3.07 ± 0.63
3.6822	51.0 ± 0.7	70.3 ± 10.9	0.1 ± 0.0	22.69 ± 0.03	6.07 ± 0.95	4.08 ± 0.67
3.6826	51.2 ± 0.7	113.2 ± 13.2	0.1 ± 0.0	22.51 ± 0.04	9.82 ± 1.15	5.29 ± 0.71
3.6834	51.8 ± 0.7	195.9 ± 17.5	0.3 ± 0.0	22.25 ± 0.04	16.98 ± 1.54	5.47 ± 0.58
3.6840	50.7 ± 0.7	418.6 ± 24.3	0.7 ± 0.0	22.15 ± 0.05	37.21 ± 2.23	9.35 ± 0.63
3.6846	48.7 ± 0.7	609.8 ± 29.6	1.2 ± 0.0	22.11 ± 0.05	56.50 ± 2.87	15.14 ± 0.82
3.6848	39.9 ± 0.6	717.9 ± 32.0	1.1 ± 0.0	22.10 ± 0.05	81.33 ± 3.86	24.74 ± 1.35
3.6854	38.0 ± 0.6	875.3 ± 35.2	1.5 ± 0.1	22.09 ± 0.05	104.00 ± 4.53	79.50 ± 7.26
3.6860	41.2 ± 0.6	961.3 ± 36.8	1.9 ± 0.1	22.08 ± 0.05	105.52 ± 4.38	1275.71 ± 160.43
3.6866	40.1 ± 0.6	916.0 ± 35.6	1.8 ± 0.1	22.09 ± 0.05	103.11 ± 4.34	85.80 ± 8.63
3.6873	40.7 ± 0.6	748.9 ± 32.5	1.4 ± 0.1	22.10 ± 0.05	83.18 ± 3.86	20.33 ± 1.13
3.6874	40.1 ± 0.6	645.2 ± 30.1	1.4 ± 0.1	22.10 ± 0.05	72.65 ± 3.59	16.34 ± 0.91
3.6890	40.7 ± 0.7	291.0 ± 20.5	0.4 ± 0.0	22.20 ± 0.05	32.19 ± 2.33	6.65 ± 0.52
3.6920	41.6 ± 0.7	107.2 ± 12.9	0.1 ± 0.0	22.48 ± 0.04	11.46 ± 1.39	3.65 ± 0.45
3.6964	49.7 ± 0.7	57.6 ± 9.9	0.1 ± 0.0	22.68 ± 0.03	5.11 ± 0.88	1.93 ± 0.33
3.7002	50.7 ± 0.7	72.7 ± 10.5	0.1 ± 0.0	22.80 ± 0.03	6.28 ± 0.91	2.64 ± 0.39
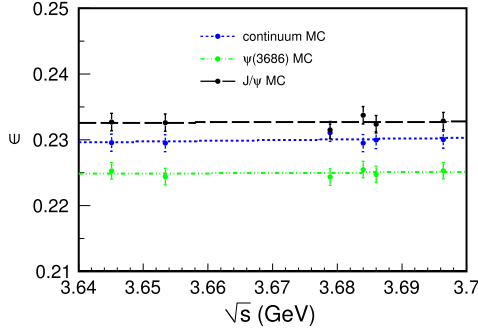
Fig. 2. Detection efficiency as a function of c.m. energy for each signal process.

in the corresponding signal MC samples. For each signal process, MC samples at six different c.m. energies are generated, and a linear dependence of the efficiency on $\sqrt{s}$ is found, as shown in Fig. 2. The efficiency values at other c.m. energies are determined by extrapolation of the respective linear fitting function. The three signal processes studied differ slightly in the angular distribution of the inclusive K_S^0. The efficiency differences visible in Fig. 2 are caused by the interplay of these angular distributions and the implicit fiducial cuts applied during event reconstruction.

To improve the reliability of the efficiency estimation, a bin-by-bin correction is applied to the K_S^0 momentum and angular distributions in the $\psi(3686)$ and continuum MC samples. No correction is made for the J/ψ samples, since the contribution of ISR J/ψ events is small in the studied energy region. In the plots (a) and (c) of Fig. 3, the distributions after the correction are shown at $\sqrt{s} = 3.686$ GeV, where the backgrounds are estimated with selection $M_{\pi^+\pi^-} \in (0.4, 0.6)$ GeV/c^2 in the MC sample. In the same figure, the plots (b) and (d) show the comparisons for continuum between the data and the MC sample at $\sqrt{s} = 3.6534$ GeV, where the backgrounds are estimated from the data sidebands $21 < |M_{\pi^+\pi^-} - M_{K_S^0}| < 42$ MeV/c^2 and the signal region is defined as $|M_{\pi^+\pi^-} - M_{K_S^0}| < 11$ MeV/c^2, where $M_{K_S^0}$ is the nominal mass of K_S^0 [3]. Good agreement between data and MC samples is observed.

The detection efficiency for the inclusive process $e^+e^- \to K_S^0 X$ at the ith c.m. energy is determined by

$$
\epsilon^i_{e^+e^- \to K_S^0 X} = \frac{1}{\sigma^i_{\psi(3686)} + \sigma^i_{J/\psi} + \sigma^i_{\mathrm{con}}} \times
$$
$$
(\sigma^i_{\psi(3686)} \cdot \epsilon^i_{\psi(3686)} + \sigma^i_{J/\psi} \cdot \epsilon^i_{J/\psi} + \sigma^i_{\mathrm{con}} \cdot \epsilon^i_{\mathrm{con}}),
\tag{11}
$$

where $\epsilon^i_{\psi(3686)}$, $\epsilon^i_{J/\psi}$ and $\epsilon^i_{\mathrm{con}}$ are the efficiencies of the signal processes determined for the ith energy point, while $\sigma^i_{\psi(3686)}$, $\sigma^i_{J/\psi}$ and σ^i_{con} are the corresponding signal cross sections obtained with an iterative procedure by fitting the measured line-shape with Eqs. (1)-(9). For the first iteration, the efficiency is estimated setting the parameters to the following initial values: Δ is set to 1.30 MeV measured [19] at $\sqrt{s} = 3.686$ GeV, f_{con} to the value estimated from the continuum data, $\mathcal{B}(R \to K_S^0 X)$ ($R = J/\psi, \psi(3686)$) to the values estimated from the J/ψ and $\psi(3686)$ signal MC samples, and the other parameters are set to PDG [3] values.

For each data sample the measured observed cross section of $e^+e^- \to K_S^0 X$ is determined by

$$
\sigma^{\mathrm{obs}} = \frac{N^{\mathrm{obs}} - N^{\mathrm{bkg}}}{\mathcal{L} \times \epsilon^{e^+e^- \to K_S^0 X}},
\tag{12}
$$

where N^{obs} is the number of observed inclusive K_S^0 events, N^{bkg} is the number of background events, $\mathcal{L}$ is the integrated luminosity and $\epsilon^{e^+e^- \to K_S^0 X}$ is the detection efficiency determined according to Eq. (11).

The observed cross section at each energy point is first obtained with the initial detection efficiency. By fitting the observed cross sections with Eq. (1), the parameters of Eqs. (2) and (3) are updated, and new detection efficiencies are calculated. The iterations are repeated until the change of the parameters is less than 0.1%. The procedure converges after three iterations. The expected contribution from J/ψ is around 0.2 nb, while the continuum contribution varies from 2.54 nb to 2.47 nb across the energy range. The final detection efficiency for $e^+e^- \to K_S^0 X$ is shown in Fig. 4 as a function of the c.m. energy. The efficiency values $\epsilon^{J/\psi}_{K_S^0 X}$, $\epsilon^{\psi(3686)}_{K_S^0 X}$, and $\epsilon^{\mathrm{con}}_{K_S^0 X}$ are estimated to be 23.27%, 22.05%, 23.54%, respectively, with little variation over the studied energy range. Since the efficiency contribution of $\psi(3686)$ gradually increases and decreases on either side of $\psi(3686)$ peak energy and the $\psi(3686)$ efficiency is lower than the continuum efficiency, the final detection efficiency with energy dependency in Fig. 4 looks like a valley. The
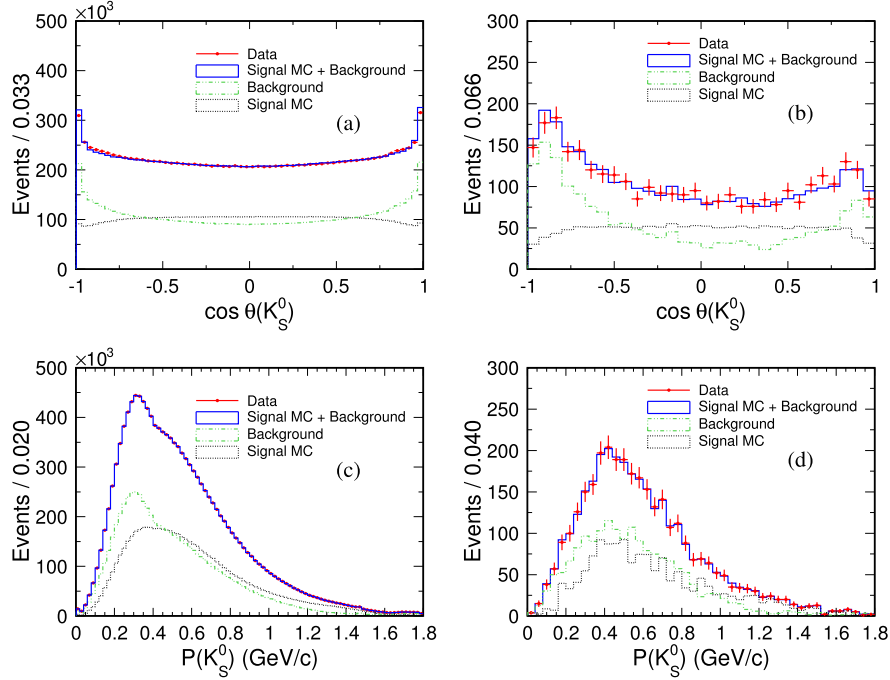
Fig. 3. Comparisons between the standard $\psi(3686)$ data and the standard $\psi(3686)$ MC sample at $\sqrt{s} = 3.686$ GeV for K_S^0 (a) angular and (c) momentum distributions after corrections. The comparisons between continuum data and continuum $K_S^0 X$ MC sample at $\sqrt{s} = 3.6534$ GeV for K_S^0 (b) angular and (d) momentum distributions after corrections. The red dots with error bars are data, the black dotted histograms are the signal MC events, the green dash-dotted histograms are the estimated background events and the blue solid histograms are the sum of signal MC events and estimated background events.
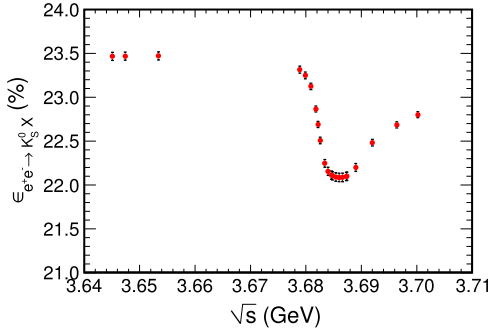
Fig. 4. Detection efficiency as a function of c.m. energy for $e^+e^- \to K_S^0 X$, where the vertical axis is expanded.

values of the detection efficiency and the observed cross sections of $e^+e^- \to K_S^0 X$ are listed in Table 2, where only statistical errors are given.

4.2. Fit to $\sigma^{obs}(e^+e^- \to K_S^0 X)$

We perform a chi-square fit to the energy dependent observed cross section determined with the iterative procedure described in the previous section. The fit allows the determination of the product of $\Gamma_{\psi(3686)}^{ee}$ and BF of $\psi(3686) \to K_S^0 X$ as described in section 2. The total expected cross sections for $e^+e^- \to K_S^0 X$ can be written as

$$\sigma_{K_S^0 X}^{obs}(s) = \sigma_{K_S^0 X}^{\psi(3686)}(s) + \sigma_{K_S^0 X}^{J/\psi}(s) + \sigma_{K_S^0 X}^{con}(s),\qquad(13)$$

which is the sum of the observed cross sections of the three main processes contributing to the final state. Any interference between resonant and continuum contribution is expected to be different in different specific channels, and is therefore expected to be negligible in the measurement of the inclusive process.

The parameters of the fit function can be divided into three groups: J/ψ parameters, $\psi(3686)$ parameters, and the remaining parameters. All the J/ψ parameters are fixed to the PDG [3] values except for the $\mathcal{B}(J/\psi \to K_S^0 X)$ which is fixed to the value estimated from the inclusive MC due to the lack of experimental measurements. Parameters of $\psi(3686)$ are free parameters of the fit, except for $\Gamma_{\psi(3686)}^{tot}$ which is fixed to the PDG values. Other parameters, f_{con} of Eq. (3) and the beam energy spread Δ are free parameters. The value of Δ is assumed to be constant in the whole energy range used in the fit.

The fit is performed using only the statistical uncertainties of the measured cross sections. The best fit result is shown in Fig. 5. The product of $\Gamma_{\psi(3686)}^{ee}$ and BF for the inclusive decay of $\psi(3686) \to K_S^0 X$ is determined to be $\Gamma_{\psi(3686)}^{ee} \mathcal{B}(\psi(3686) \to K_S^0 X) = (373.8 \pm 6.7)$ eV. In Table 3, the parameters of the best fit function are summarized. The large $\chi^2/n.d.f$ is dominated by the two points at the c.m. energies of 3.6848 and 3.6854 GeV. Without these points the $\chi^2/n.d.f$ is 27.2/16 and $\Gamma_{\psi(3686)}^{ee} \mathcal{B}(\psi(3686) \to K_S^0 X)$ changes to 365.8 eV. Assuming $\Gamma_{\psi(3686)}^{ee} = (2.33 \pm 0.04)$ keV [3], the BF for the inclusive decay of $\psi(3686) \to K_S^0 X$ is measured to be $\mathcal{B}(\psi(3686) \to K_S^0 X) = (16.04 \pm 0.29)\%$.

Table 3
Results of the fit to the observed cross sections for $e^+e^- \to K_S^0 X$.

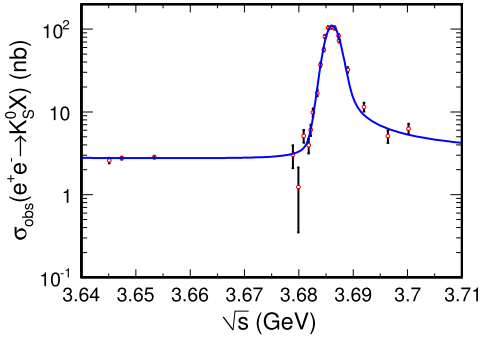| Parameter	Solution
Energy spread [MeV]	1.33 ± 0.03
f_{con}	28.49 ± 0.80
$M_{J/\psi}$ [MeV/c^2]	3096.9 (fixed)
$\Gamma_{J/\psi}^{tot}$ [keV]	92.9 (fixed)
$\Gamma_{J/\psi}^{ee} \mathcal{B}(J/\psi \to K_S^0 X)$ [eV]	941.28 (fixed)
$M_{\psi(3686)}$ [MeV/c^2]	3686.03 ± 0.03
$\Gamma_{\psi(3686)}^{tot}$ [keV]	294 (fixed)
$\Gamma_{\psi(3686)}^{ee} \mathcal{B}(\psi(3686) \to K_S^0 X)$ [eV]	373.8 ± 6.7
$\chi^2/n.d.f$	45.3/18

Fig. 5. Best fit to the observed cross sections for $e^+e^- \to K_S^0 X$. The red dots with error bars are the measured cross sections, and the blue line is the fit result.

5. Systematic uncertainties

The systematic uncertainties on $\Gamma_{\psi(3686)}^{ee} \mathcal{B}(\psi(3686) \to K_S^0 X)$ originate mainly from the measurement of the observed cross sections for $e^+e^- \to K_S^0 X$, the fitting procedure and the uncertainties of the c.m. energy.

The systematic uncertainties for the measurement of the observed cross sections arise from the following sources: (1) event selection (N_{good}, R_{xy} and R_z requirements); (2) K_S^0 reconstruction; (3) uncertainty of the integrated luminosity, 1.00% from Ref. [20]; (4) uncertainty on $\mathcal{B}(K_S^0 \to \pi^+\pi^-)$, 0.07% from the PDG [3]; (5) fit to $M_{\pi^+\pi^-}$; (6) MC modeling; and (7) background subtraction. For the sources (1), (5), (6) and (7), the uncertainties are evaluated by re-measuring the cross section with the changes described below. The largest deviations from the nominal results are taken as systematic uncertainties.

For source (1), the selection requirements are changed from $N_{\text{good}} > 2$ to $N_{\text{good}} \geq 2$, and for the tracks not originating from K_S^0 from $R_{xy} < 1.0$ cm and $R_z < 10.0$ cm to $R_{xy} < 10.0$ cm and $R_z < 20.0$ cm. The measured observed cross section changes by 0.67% and 2.87%, respectively. Source (2) is studied using a control sample of $J/\psi \to K^*(892)^\pm K^*(892)^\mp$ and $K^*(892)^\pm \to K_S^0 \pi^\pm$ events collected at $\sqrt{s} = 3.097$ GeV. The estimated uncertainty is 2.09%. To study source (5) we vary the fit range, the bin width, the signal shape and the background shape. Adding the changes of the result in quadrature, the uncertainty is 3.32%. For source (6), the selection efficiency is evaluated from the MC samples excluding events where the K_S^0 did not originate from a K^0 meson according to the generator information. The observed change of cross section, 1.51%, is taken as the systematic uncertainty. For source (7), the $K_L^0 + Y$ production cross section is replaced by the measured $K_S^0 + X$ cross section, and the change of the BF by 0.04% is taken as the systematic uncertainty.

The relative uncertainties in the measurement of the observed cross section are listed in Table 4 for all sources described above. Assuming they are independent, the total value of 5.23% is obtained by adding them in quadrature according to the "offset method" [21].

The systematic uncertainties of the fit procedure arise from the fixed parameters, the continuum parametrization and the energy spread Δ. They are evaluated by repeating the fitting procedure with changes detailed below and taking the difference with the nominal result of $\Gamma_{\psi(3686)}^{ee} \mathcal{B}(\psi(3686) \to K_S^0 X)$ as the systematic uncertainty. For the fixed parameters the largest uncertainties is from $\Gamma_{\psi(3686)}^{\text{tot}}$. By changing the parameter by $\pm 1\sigma$ of the PDG error [3] the systematic uncertainty is evaluated to be 0.12%. The contribution from the fixed J/ψ parameters is negligible. The uncertainty from the continuum parametrization is evaluated by changing the expression of Eq. (3), to $\sigma_{K_S^0 X}^{\text{con}} = f_{\text{con}}/s^n$ and repeating the fit procedure with n as a free parameter. The resulting systematic uncertainty is found to be 0.06%. For the beam energy spread Δ the uncertainty is estimated replacing the value obtained from the fit by the nominal value 1.30 MeV obtained with the beam energy measurement system [19]. The change of 0.68% in $\Gamma_{\psi(3686)}^{ee} \mathcal{B}(\psi(3686) \to K_S^0 X)$ is assigned as the systematic uncertainty.

The systematic uncertainty due to the c.m. energy is estimated by changing the energy values within the errors [19] and re-fitting the observed cross sections. The uncertainty is estimated to be 0.87%.

Assuming that all the contributions listed above are independent, the total uncertainty for measuring $\Gamma_{\psi(3686)}^{ee} \mathcal{B}(\psi(3686) \to K_S^0 X)$ is estimated by adding them in quadrature and is found to be 5.35%, as summarized in Table 5.

Table 4
Systematic uncertainties for measuring the observed cross sections (σ^{obs}) of $e^+e^- \to K_S^0 X$ in %.

Source	Systematic uncertainty
N_{good}	0.67
$R_{xy} < 1.0$ cm and $R_z < 10.0$ cm	2.87
K_S^0 reconstruction	2.09
$\mathcal{L}$	1.00
$\mathcal{B}(K_S^0 \to \pi^+\pi^-)$	0.07
Fit to $M_{\pi^+\pi^-}$	3.32
MC modeling	1.51
Background subtraction	0.04
Total	5.23

Table 5
Systematic uncertainties for measuring the product of $\Gamma_{\psi(3686)}^{ee}$ and branching fraction of $\psi(3686) \to K_S^0 X$ in %.

Source	Systematic uncertainty
σ^{obs}	5.23
Fixed fit parameters	0.12
Continuum parametrization	0.06
Δ	0.68
$\sqrt{s}$	0.87
Total	5.35

6. Summary

The observed cross sections for $e^+e^- \to K_S^0 X$ (where $X =$ anything) are measured at 22 energy points in the range from 3.640 to 3.701 GeV using the data collected by BESIII detector at the BEPCII Collider. By fitting the observed cross sections as a function of the c.m. energy, the product of $\Gamma_{\psi(3686)}^{ee}$ and BF of $\psi(3686) \to K_S^0 X$ is measured for the first time to be $\Gamma_{\psi(3686)}^{ee} \mathcal{B}(\psi(3686) \to K_S^0 X) = (373.8 \pm 6.7 \pm 20.0)$ eV, and assuming $\Gamma_{\psi(3686)}^{ee} = (2.33 \pm 0.04)$ keV [3], the BF of $\psi(3686) \to K_S^0 X$ is determined to be

$$\mathcal{B}(\psi(3686) \to K_S^0 X) = (16.04 \pm 0.29 \pm 0.90)\%, \qquad (14)$$

where the first uncertainty is statistical and the second is systematic, combining the error of $\Gamma_{\psi(3686)}^{ee}$ into the systematic error. The sum of all the BFs of $\psi(3686)$ decays to exclusive K_S^0 final states including the transitions followed by J/ψ and χ_{cJ} ($J = 0, 1, 2$) decays is $\sim 5.95\%$ as reported in the PDG [3], which is much lower than the current measurement. This suggests that there are many undiscovered exclusive channels for $\psi(3686)$ decay to final states containing K_S^0.

Declaration of competing interest

The authors declare that they have no known competing financial interests or personal relationships that could have appeared to influence the work reported in this paper.

Acknowledgements

References

[1] W. Kwong, Phys. Rev. D 37 (1988) 3210.
[2] G.S. Abrams, et al., Phys. Rev. Lett. 33 (1974) 1453.
[3] M. Tanabashi, et al., Particle Data Group, Phys. Rev. D 98 (2018) 030001.
[4] G.S. Abrams, et al., Phys. Rev. Lett. 34 (1975) 1181.
[5] J.E. Gaiser, et al., Phys. Rev. D 34 (1986) 711.
[6] M. Ablikim, et al., BES Collaboration, Phys. Lett. B 641 (2006) 145.
[7] E.A. Kuraev, V.S. Fadin, Yad. Fiz. 41 (1985) 733.
[8] M. Ablikim, et al., BESIII Collaboration, Nucl. Instrum. Meth. A 614 (2010) 345.
[9] C.H. Yu, et al., in: Proceedings of IPAC2016, Busan, Korea, 2016.
[10] S. Jadach, B.F.L. Ward, Z. Was, Phys. Rev. D 63 (2001) 113009.
[11] D.J. Lange, Nucl. Instrum. Meth. A 462 (2001) 152;
     R.G. Ping, Chin. Phys. C 32 (2008) 599.
[12] J.C. Chen, G.S. Huang, X.R. Qi, D.H. Zhang, Y.S. Zhu, Phys. Rev. D 62 (2000) 034003.
[13] S. Agostinelli, et al., GEANT4 Collaboration, Nucl. Instrum. Meth. A 506 (2003) 250.
[14] Y. Liang, B. Zhu, Z. You, et al., Nucl. Instrum. Meth. A 603 (2009) 325.
[15] Z.Y. You, Y.T. Liang, Y.J. Mao, Chin. Phys. C 32 (2008) 572.
[16] G. Balossini, C.M. Carloni Calame, G. Montagna, O. Nicrosini, F. Piccinini, Nucl. Phys. B 758 (2006) 227.
[17] M. Ablikim, et al., BESIII Collaboration, Chin. Phys. C 37 (2013) 063001.
[18] M. Xu, et al., Chin. Phys. C 33 (2009) 428.
[19] M.N. Achasov, N.Yu. Muchnoi, J. Instrum. 12 (2017) C08007.
[20] M. Ablikim, et al., BESIII Collaboration, Chin. Phys. C 37 (2013) 123001.
[21] M. Botje, J. Phys. G, Nucl. Part. Phys. 28 (2002) 779.